International Journal of Engineering Trends and Technology
ISSN: 2231–5381 / https://doi.org/10.14445/22315381/IJETT-V73I4P103

Volume 73 Issue 4, 24-33, April 2025

Original Article

GPR Image Classification of Buried Objects using Deep Learning with Attention Mechanism

T. Kalaichelvi[1], S. Ravi[2], Buddepu Santhosh Kumar[3]

[1,2]Department of Computer Science, Pondicherry University, Puducherry, India.
[3]Department of Electronics and Communication Engineering, Amrita Vishwa Vidyapeetham, Andhra Pradesh, India.

[2]Corresponding Author : sravicite@pondiuni.ac.in

Received: 23 July 2024 Revised: 11 February 2025 Accepted: 06 March 2025 Published: 26 April 2025

Abstract - *The contamination of landmines and other unexploded ordnances has become a global safety problem. There is an urgent need to identify and demine the buried unexploded ordnance from the subsurface to save people and civilians from severe injury and death. Ground Penetrating Radar (GPR) is the best geophysical imaging technique for identifying and recognizing underground objects. It retrieves large GPR B-Scan datasets from the subsurface to be processed and classified using deep learning techniques. The proposed technique describes GPR B-Scan images of buried objects like landmines with casing materials made of metal and plastic, which can be classified using deep learning with attention mechanisms with MobileNetV2 as the base model. It uses deep learning architecture to successfully extract essential features and recognize them from GPR images of metal pipes, metal tiffin boxes, and plastic tiffin boxes. It includes creating novel datasets on gprMax software with the real-time scenario of a homogeneous medium, added roughness, water, and grass to support a heterogeneous soil medium with different relative permittivity, casing material, object size, and burial depth. The process initiates with the preprocessing of GPR data, applying data augmentation, splitting the datasets into training and testing, and building a deep learning architecture with attention mechanism; finally, training the network model and testing for GPR image classification. The multi-class classification evaluated and showcased improved performance using deep learning with attention mechanism than traditional methods. The developed model can potentially support new inventions in archaeology, infrastructure assessment, and explosive ordnance identification.*

Keywords - *Attention mechanism, Buried object, Data augmentation, Deep learning, Ground penetrating radar, Image classification, Landmine, MobileNetV2.*

1. Introduction

Ground Penetrating Radar (GPR) is an imaging technique of subsurface investigation utilized in archaeology, remote sensing, environmental science, military, and civil engineering applications [1]. The GPR data is analyzed by extracting features from images or manually interpreting them using machine learning techniques, which are time-consuming and impossible to handle massive datasets efficiently. Deep learning is the subfield of machine learning that takes the capabilities of Artificial Neural Networks (ANN), which consists of a number of layers that interact with one another to make predictions.

Deep learning technique with unique architecture automatically extracts the essential features from data and achieve the best outcomes for detection and classification. It analyzes images and processes voices without relying on human-defined features. It can detect image boundaries, patterns, objects, and complete scene elements. The vast collection of tools accessible in deep learning allows the processing of different data formats. Object identification uses Convolutional Neural Networks (CNNs) to manage images and videos. A convolutional combination with pooling operations enhances image feature extraction for image analytical purposes. Recurrent Neural Networks (RNNs) are highly effective in performing sequential data measurement tasks because they can assess information series and relations in time, such as speech and text. Generative Adversarial Networks (GANs) enable data expansions because they produce entirely new data sets.

The networks include generators that produce new information and discriminators that distinguish real from artificial data and then develop realistic results. Transformers have completely reformed natural language processing because they can identify word relationships throughout entire sequences of words. The faster operation and superior performance of transformers contrast positively with RNNs because the networks do not need to process information sequentially. Multiple approaches within deep learning led to its powerful ability to help solve various complex problems. CNN has gained significant popularity with deep learning approaches during the last few years, thereby revolutionizing GPR image evaluations [2] [3] [4].

This exceptional combination allows CNNs to learn hierarchical representations directly from GPR data. CNNs can identify subsurface structures and materials more precisely by doing this since they can recognize complex patterns and characteristics within the images. The usage of small labeled data sets and data augmentation used to resolve GPR B-scan data variability. The modified model achieves better results and higher accuracy in detecting anomalies along with subsurface geological formations.

However, the standard deep learning approaches cannot focus on spectral and spatial features in GPR images utilized for classification. Attention methods, including spatial and channel attention, provide reliable solutions to concentrate on the discriminative parts of GPR images while automatically updating feature importance. Attention mechanisms are used in remote sensing tasks [5] [6] and medical image processing for diagnosis of disease and treatment [7] [8] to improve image classification. The successful implementation of attention-based models in natural image processing remains insufficient, and minimal models in subsurface object investigations and landmine detection.

2. Literature Survey

Various researchers have investigated deep learning approaches as tools to analyze GPR B-Scan image data. Table 1 demonstrates the GPR technology for buried object classification using deep learning techniques, which includes the details of the method employed, the object preferred for classification, the dataset utilized, and limitations of the technique with accuracy or loss functions achieved.

Giovanneschi et al. [9] used support vector machines (SVMs) for the classification of landmine targets with decreased learning times (LT) by using online dictionary learning (ODL) techniques. Darknet-53 employed by Zong et al. [10] and Liu et al. [11] used You Only Look Once version 3 (YOLOv3) for underground object classification and datasets collected from various sources such as wells, cables, steel reinforcement, metal and nonmetal pipes. Using neural networks (NN), Smitha et al. [12] differentiated buried mines from clutter using GPR images of buried mines, including geometric and statistical properties.

Lei et al. [13] used CNN with long short-term memory (LSTM) to identify hyperbolic shapes of buried objects. Underground object identification and improvised landmines include Faster region convolutional neural networks (Faster R-CNN) [14], with deep CNN [15] [16], and deep reinforcement learning (DRL) [17] as well as deep neural networks (DNN) [18]. The research conducted by Jaufer et al. [19] with wavelet-based pipeline detection procedures included data augmentation [20] for edge detection functionality of the pipeline [21]. Sezgin et al. [22] used CNN for two-class Classification of metallic and non-metallic anti-personnel surrogate mines.

The research presents specific insights about deep learning applications for GPR B-Scan image classification of buried objects through various processes to automate exploration techniques. GPR technology has received significant improvements by integrating artificial intelligence technologies into geophysics operations. Notably, a CNN-LSTM [13], Deep CNN [15] [16], and CNN [20], [22] needed high computational resources to train on specific datasets. In highly cluttered environments, RCNN [14] or a DNN-based [18] technique will fail, resulting in false detections, and due to small or non-diverse datasets, most approaches will overfit. Deep learning architecture combined with attention is primarily used to classify images. Standard CNN takes into consideration every section of image input. The model's Attention mechanism methods solve this issue through selective feature extraction in targeted image areas to improve classification accuracy.

A model improvement technique applies attention layers, determining weight distribution according to essential feature levels. Attention-based processing systems enable better detection of subsurface elements through GPR and other imaging technologies. Table 2 shows attention mechanism-based object classification in deep learning, which includes the details of the classification method employed, the object preferred for classification, the attention mechanism involved, and the dataset utilized with the accuracy achieved.

Su et al. [23] built a deep learning model with attention mechanisms to analyze significant points. Meng et al. [24] integrated channel and spatial attention allow extraction of more valuable features by focusing on crucial places within GPR images. Ullah et al. [25] created a dense attention mechanism called DenseNet for COVID-19 identification by utilizing chest X-rays. Zheng et al. [26] used RebarNet with attention technique to handle erroneous and false detections involving tiny object detection.

Zhang et al. [27] approach significantly reduced the influence of unnecessary data by addressing the difficulties of RTS images by depth residual shrinkage network (DRSNet) with an attention mechanism. Huang et al. [28] classified rock, incorporating a triplet attention mechanism for increased accuracy using EfficientNet. Furthermore, a network known as a double-branch multi-scale dual-attention (DBMSDA) was presented by Zhang et al. [29] to extract spatial and also spectral features of hyperspectral images (HSI) using multi-scale spectral residual self-attention (MSeRA). TransUNet was used with self-attention for performance enhancement in GPR inversion tasks by Junkai et al. [30].

Table 1. GPR Technology for buried object classification using deep learning

Author	Method	Classification	Dataset	Limitations	Accuracy
Giovanneschi et al., [9]	SVM	Landmine	Real	Complex soil conditions are difficult to generalize	LT-93%
Zong et al., [10]	Darknet-53	Underground object	Real	Limited capability to identify different types of objects	89.2%
Liu et al. [11]	YOLOv3	Underground pipeline	Real	Struggles with small and irregularly shaped objects	95.6 %
Smitha et al., [12]	NN	Landmine	Surrogate	Overfitting due to limited training data	95%
Lei et al., [13]	CNN-LSTM	Buried object	Simulated	High computational cost in sequential processing	99.5%
Gong et al., [14]	Faster RCNN	Underground object	Simulated	Poor depth estimation and localization accuracy	93.9%
Kim et al. [15]	Deep CNN	Underground object	Real	Struggle to identify objects in cluttered environments	98%
Wang et al., [16]	Deep CNN	Buried target	Simulated	Struggle soil and subsurface variations	93.23%
Omwenga et al., [17]	DRL	Subsurface Object	Simulated	Lacks a standardized dataset for proper evaluation	ROI -3.56
Mahmood et al. [18]	DNN	Landmine	Simulated	Produce a high false positive rate in specific scenarios	89.46%
Jaufer et al., [19]	SVR	Buried pipe	Simulated	Limited evaluation of real-world conditions	MARE-0.39%
Bai et al. [20]	CNN	Underground pipeline	Simulated	Depth estimation error	97.35%
Mizutani et al. [21]	Edge	Subsurface pipe	Real	Accuracy depends on high-quality preprocessing	AE- 0.1175
Sezgin et al., [22]	CNN	Anti-personnel mine	Surrogate	Struggle to identify different buried object	98%

Table 2. Object classification using deep learning with an attention mechanism

Author	Method	Classification	Attention Mechanism	Dataset	Accuracy
Su et al., [23]	Darknet53	Buried utilities	Channel attention	Real Data	97.01%
Meng et al., [24]	Few-shot	Image	Channel and spatial attention	miniImageNet and omniglot	68.28%
Ullah et al., [25]	DAM-Net	COVID-19	Densely attention	COVIDx	97.22%
Zheng et al., [26]	RebarNet	Rebar	Embedded attention	Open-source	97.9%
Zhang et al., [27]	DRSNet	Rock	Channel attention	Open-source	93.69%
Huang et al., [28]	EfficientNet	Rock	Triplet attention	ImageNet	93.2%
Zhang et al., [29]	DBMSDA	Hyperspectral image	Spectral residual self-attention	Geological Lithology hyperspectral	74.13%
Junkai et al., [30]	TransUNet	Subsurface defects	Regressive self-attention	Simulated data	-

Attention mechanisms employed in [24], [26], [28], and [30] lacked comparisons with traditional methods, which have to strengthen with feature extraction methods, and [25], [27], and [29] need to discuss the performance achieved and increased computational complexity extensively. Although [23] and [30] applied attention to GPR and hyperspectral imaging, they failed to show that attention mechanisms outperform conventional feature selection. Attention mechanisms can enhance feature extraction, as the study highlights and proved the result in different image classifications with deep learning approaches. However, its benefits in specific GPR image classification and object detection require further clarification. The research demonstrates that enhanced GPR image analysis needs collaboration between various scientific fields to achieve upcoming advancements.

3. Novel GPR Dataset

Ground penetrating radar signals of buried objects are strongly affected by the dielectric properties of soil, particularly their relative permittivity and conductivity. According to [11], soil composition and moisture content affect signal attenuation, which makes deep-learning models less capable of identifying buried objects in wet and clay soil.

The variations in soil type also caused inconsistencies in the data and affected classification accuracy [15]. Object localization and segmentation are affected by misclassifications caused by uneven surfaces and rough terrain [21]. Vehicle-borne The GPR system becomes unreliable because nearby sources and interference disrupt its operation [10]. Models of cognitive GPR using reinforcement learning attempt self-adaptation across different environments yet struggle with unknown terrain conditions, according to [17]. The particular dataset training conducted in [22] results in models that demonstrate a limited ability to work across different environments.

Figure 1 displays a pictorial illustration of the simulation process using the gprMax open-source software. As mentioned in Table 3, the simulation of the subsurface objects involved three targets: a metal pipe, a metal box, and a plastic box, which has homogeneous medium, added roughness, water, and grass to support a heterogeneous soil medium with different relative permittivity ranging from 2.5 to 10, varying casing material, 17 distinct soil types for metal pipe and box, 13 distinct soil types for a plastic box with four different sizes and seven different depths at the subsurface to overcome the problems in existing datasets.

The input file is created and executed in the Anaconda prompt under the gprMax simulation tool to get a GPR B-scan image by 30 iterations of A-Scan traces. The simulation is visualized using Paraview software based on the vti file created in the Anaconda prompt.

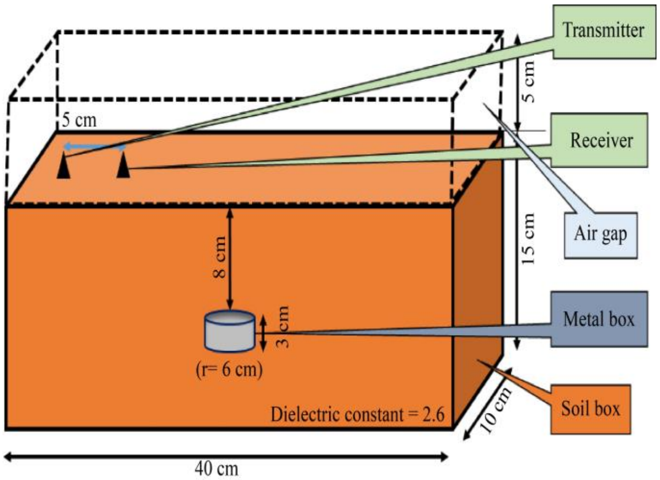

Fig. 1 Simulated data generation through gprMax

Table 3. Simulation of metal pipe and box and plastic box

Simulation Parameter	Simulation Value
Targets	Metal Pipe, Metal Box, Plastic Box
Box Dimensions	40 × 10 × 20 cm³
Air Gap	5 cm
Depth of Sand	15 cm
Antenna Movement	1-cm steps
Scanning Range	7 to 38 cm
Transmitted Pulse	Gaussian Signal
Center Frequency	2 GHz
Time Window	5 ns
Object Sizes	4 sizes: 1 cm to 4 cm diameter
Burial Depths	7 depths: 1 cm to 7 cm (1-cm intervals)
Soil Types	17 types of Metal Pipe and Metal Box 13 types of Plastic Box
Relative Permeability	$\mu_r = 1$
Relative permittivity (ϵ_r)	Ranges from 2.5 to 10 with 0.5 increments

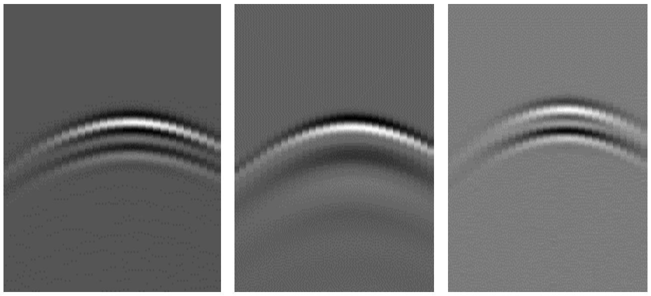

Fig. 2 B-Scan image of a single metal pipe, metal box, and plastic box

The dataset has 1200 instances, including three materials under different conditions: homogeneous, rough surface, water, and grass, each of 100 datasets. Figure 2 displays the sample B-Scan image of a single metal pipe, metal box, and plastic box. The parameters of object size, burial depth, soil type, and relative permittivity of the soil and the objects vary to get a more simulated dataset.

4. Methodology

CNN-based and Deep learning with an attention mechanism are the methods used for GPR B-scan image classification. Figure 3 specifies the CNN-based classification process for the GPR dataset, and Figure 4 shows an attention mechanism-based classification process.

The methodology explains the procedure from dataset acquisition, data augmentation, importing libraries and frameworks, and preprocessing techniques, followed by the building of the CNN model and the attention model.

4.1. CNN-Based Classification

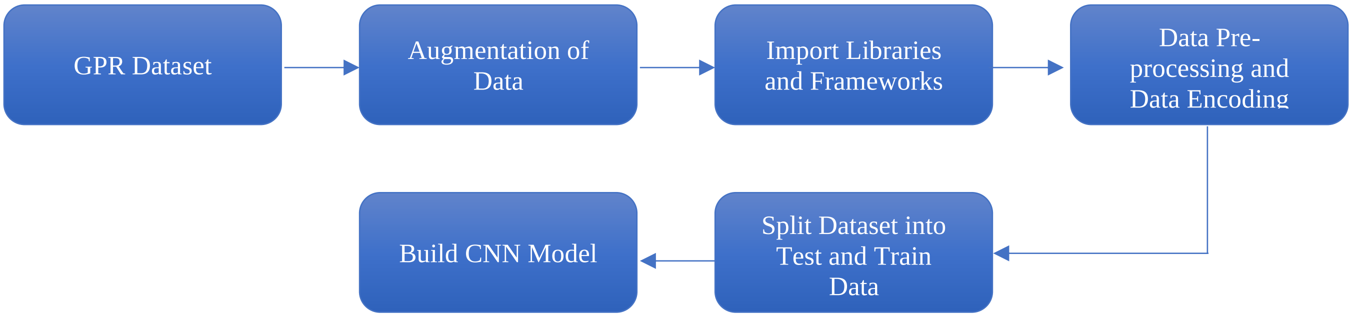

Fig. 3 Block diagram for CNN-based classification of GPR images

1. GPR Dataset: Initially, GPR images are acquired using gprMax [27]. After obtaining the dataset, the process proceeded with further techniques to classify the data.
2. Data Augmentation: The model only sees the exact orientation of the GPR image of a buried object during training; it may fail to recognize the object when it appears rotated, shifted, or zoomed in a real-world scenario. Data augmentation exposed the original input image to many variations to improve its robustness and accuracy. Augmentation includes different techniques applied to the dataset, such as image rotated 20 degrees using rotation_range = 20, shifting the image horizontally using width_shift_range = 0.2 and using height_shift_range = 0.2, and horizontal flipping, and zooming in on the image by up to 20% using zoom_range=0.2. It adds data variability and enhances the dataset to improve generalization during training. It also helps the neural network discover significant patterns in various orientations and situations by entirely capturing the underlying data.
3. Importing Libraries and Frameworks: NumPy, matplotlib, OS, cv2, sklearn, TensorFlow, and Keras are the Python libraries to import different functionalities in the Google Colab cloud platform and Python.
4. Preprocessing: It increases data consistency and the ability to extract significant features, prevent overfitting, and separate training from testing. The input image is modified using resize () to a fixed size of 224 x 224 pixels for the deep learning model. When normalizing images, the pixel values are divided by 255 to modify from 0 to 255-pixel values into 0 to 1 numerical range values. It enables the CNN model to learn more effectively and the training process to become more stable. The preprocessed images give the label list as the class name, which provides input for multi-class classification.
5. Build the CNN Model: Before building the classification model, split the dataset for training and testing with a ratio of 80,20 percent. CNN is used to extract features of GPR images through convolutional layers with filter and activation functions, and finally, it classifies the input images into different categories using output layers. The training procedure includes loss function to direct learning, batch size of 32, over 100 epochs, applying to Adam optimizer with ReLU activation function to modify parameters for the best outcomes.

4.1.1. Pseudo code for GPR B-Scan Image Classification using Deep Learning

1. pre_data = preprocess(data)
2. labels = label_encoder.fit_transform(labels)
3. X_train, X_test, y_train, y_test = train_test_split(pre_data, labels)
4. model = keras.Sequential( )
5. model.compile(optimizer='RMSprop' or 'Adam')
6. history = model.fit(datagen.flow(X_train, y_train))
7. test_loss, test_accuracy =evaluate_model(model, X_test, y_test)
8. plot(history.history['accuracy'], label=' Accuracy')
9. plot(history.history['val_accuracy'], label='Val Accuracy')

4.2. Attention Mechanism-Based Classification

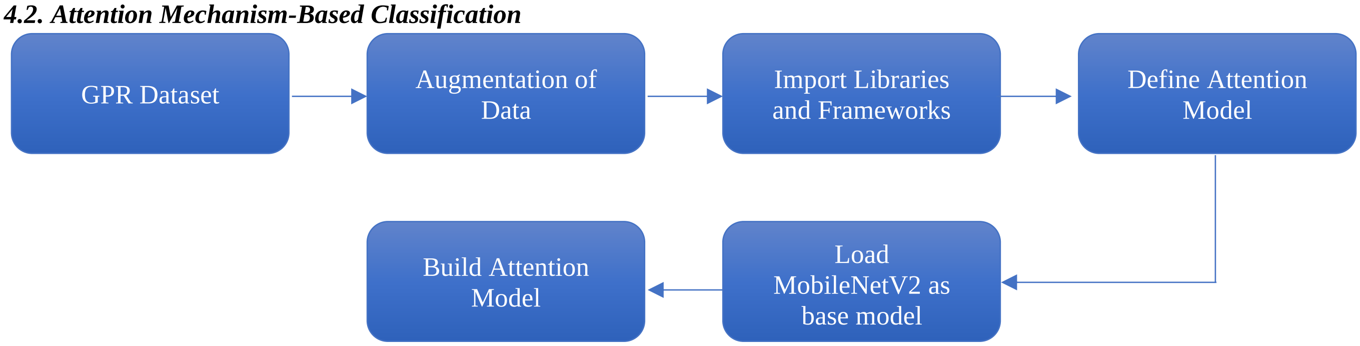

Fig. 4 Block diagram for attention mechanism-based classification of GPR images

1. GPR Dataset, Data Augmentation, and Importing Libraries and Frameworks: The same procedure has been used, like CNN-based Classification, to retrieve the GPR dataset, apply data augmentation, and import libraries and frameworks to perform various functionalities like CNN-based classification.
2. Define Attention Model: The attention model for neural networks initialized with attention types such as self-attention or multi-head attention to develop the attention layer. The system builds correlations between feature dimensions and creates trainable weight matrices based on the query, the key, and the value in the input. The attention scores are calculated to represent the input by doing the dot product between the query and the value, which represents the input. The computed scores of the GPR input image are normalized using the softmax function, making them probability distributions to describe the importance of each feature. Finally, the output is generated by performing a weighted sum of the values using the attention scores, highlighting the most relevant information.
3. Load Base Model: Load MobileNetV2 from ImageNet, eliminating classification layers as a feature extractor.
4. Build Attention Model: MobileNetV2 incorporates a self-attention mechanism to improve feature extraction from GPR images of buried objects by retrieving relevant data related to the reflected pattern of the hyperbola signature. The pre-trained model is frozen to hold the feature by applying average pooling and reshaping, then passed through a self-attention layer to enhance the informative regions of the GPR images. The attention-weighted features are then flattened using a dense layer with rectified linear unit (ReLU) activation for nonlinearity, dropout for regularization that represents further feature refinement, and finally, a dense layer classified into three object categories using a softmax activation function.

4.2.1. Pseudo code for GPR B-Scan Image Classification using Attention Mechanism

1. super (AttentionLayer, self). __init__(**kwargs)
2. super (AttentionLayer, self). build(input_shape)
3. base_model = MobileNetV2(weights='imagenet')
4. attention_model = build_attention_model(base_model)
5. attention_model.compile(optimizer='adam')
6. test_datagen = ImageDataGenerator(rescale=1. /255)
7. train_generator = train_datagen.flow_from_directory()
8. history = attention_model.fit(train_generator)
9. loss, accuracy = attention_model.evaluate(test_generator)
10. plot(history.history['accuracy'], label='Accuracy')
11. plot(history.history['val_accuracy'],label='Val_Accuracy')

5. Results

The results varied based on the parameters utilized in the deep learning model, including training the model based on the number of epochs, optimization processes, and activation functions. The CNN model accuracy is calculated using RMSProp and Adam optimizer with activation functions such as Sigmoid, Tanh, and ReLU with 5, 10, and 100 numbers of epochs to get a good accuracy level.

As shown in Table 4, CNN-based classification achieved good accuracy when the Adam optimizer with ReLU action function with 100 epochs and batch size of 32 was used.

Figure 5 displays the confusion matrix of CNN-based classification of GPR images ideally classified as 73 metal_box, 85 metal_pipe, and 69 plastic_box out of 240 (80 test cases each). Figure 6 shows the accuracy of training and validation and the loss of CNN-based classification.

Table 4. CNN-based classification accuracy based on different optimizers, activation, and epoch

Optimization Process	Activation Function	Number of Epoch	Accuracy
RMSProp	Sigmoid	5	33.33%
RMSProp	Sigmoid	10	36.25%
RMSProp	Tanh	5	33.33%
RMSProp	Tanh	10	30.42%
RMSProp	ReLU	5	86.25%
RMSProp	ReLU	10	80.83%
Adam	Sigmoid	5	30.42%
Adam	Sigmoid	10	30.42%
Adam	Tanh	5	30.42%
Adam	Tanh	10	30.42%
Adam	ReLU	5	74.17%
Adam	ReLU	10	87.92%
Adam	ReLU	100	94.58%

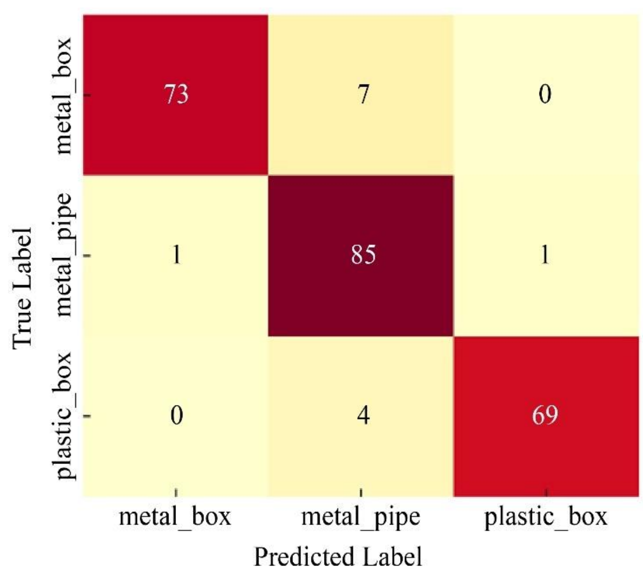

Fig. 5 Confusion matrix for CNN-based classification of GPR images

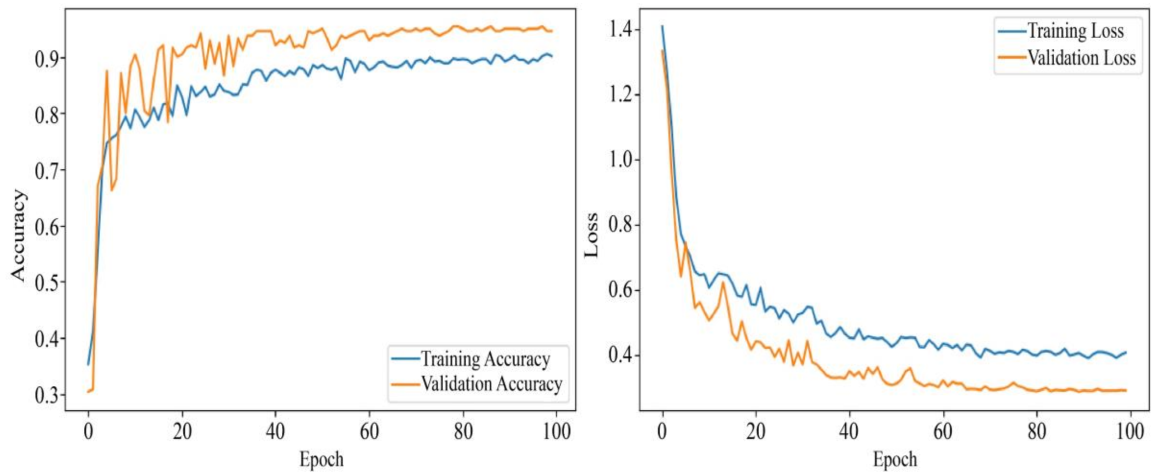

Fig. 6 Accuracy for CNN-based classification of GPR images

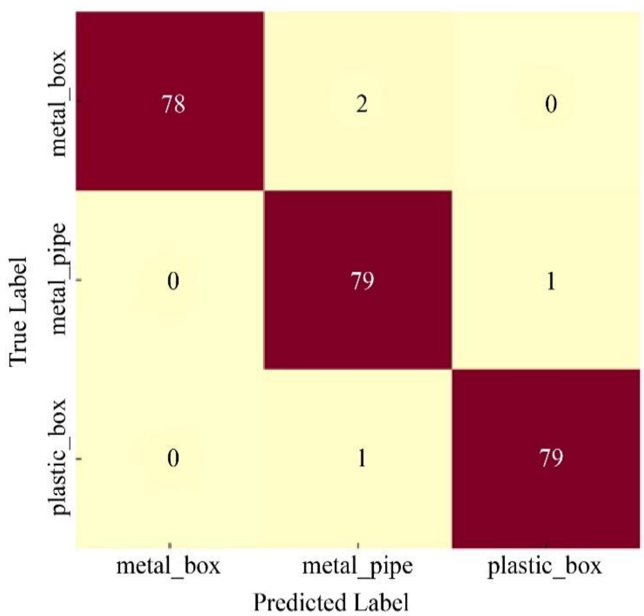

Fig. 7 Confusion matrix for Attention Mechanism with MobileNetV2

Figure 7 displays the confusion matrix of attention-based classification of GPR images ideally classified as 78 metal_box, 79 metal_pipe, and 79 plastic_box out of 240 (80 test cases each). Figure 8 illustrates the training and validation accuracy and loss of attention-based classification. Table 5 displays the classification accuracy of metal_box, metal_pipe, and plastic_box using CNN, as well as the attention mechanism.

Table 5. Classification accuracy CNN, MobileV2 Net with Attention Mechanism based on Adam optimizers, ReLU activation

Model	Performance Metric	Metal Box	Metal Pipe	Plastic Box
CNN	Precision	0.99	0.89	0.99
	Recall	0.91	0.99	0.95
	F1-Score	0.95	0.93	0.96
	Accuracy	**94.58%**	**94.58%**	**94.58%**
MobileNetV2 with Attention Mechanism	Precision	1.00	0.96	0.99
	Recall	0.98	0.99	0.99
	F1-Score	0.99	0.98	0.99
	Accuracy	**99.23%**	**99.23%**	**99.23%**

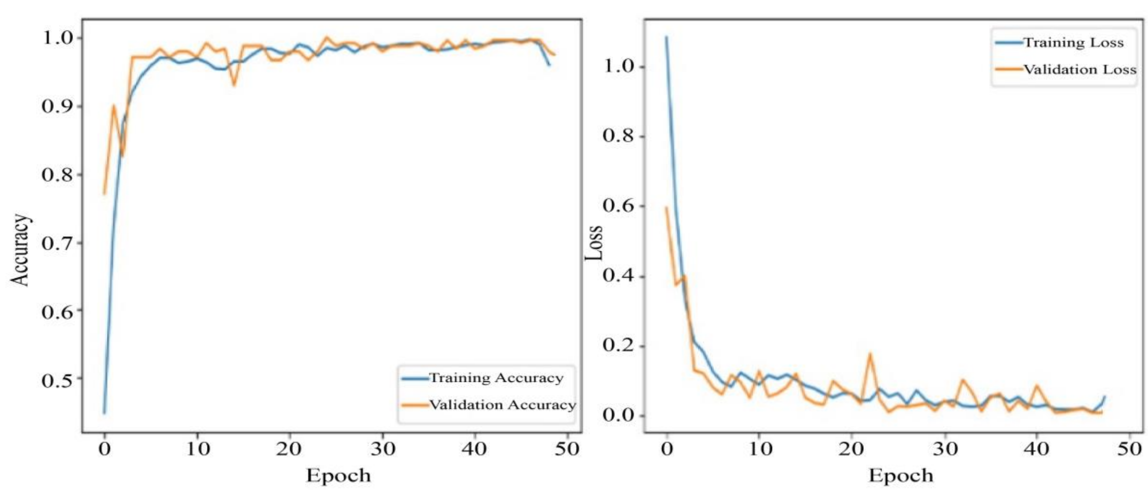

Fig. 8 Accuracy of deep learning with an attention mechanism

6. Discussions

Ground penetrating radar images of landmine classified through a deep learning model achieving 94.58% accuracy using the ReLU activation to ensure more consistent convergence and avoid vanishing gradient issues of training; Adam optimizer enhances training speed and reduces overfitting and batch size of 32 over 100 epochs enhances computational efficiency and accelerates training; however, it may sometimes compromise model generalization. However, it achieved the highest accuracy depending on GPR B-scan dataset characteristics, model architecture, and the nature of the image classification problem. The outstanding accuracy accomplished is highly dependent on the characteristics of the GPR image dataset, the CNN model architecture, and the complexity of the classification task. The performance of deep learning models heavily depends on using suitable hyperparameters to obtain maximum results when implementing different factors. Figure 9 shows the comparison of the existing deep learning model with the proposed model for buried object classification. Also, it is classified as 85 metal_pipe, but the total test cases are given as 80 for metal_pipe. The MobileNetV2 architecture functions as a mobile and computer vision application that maintains lightweight requirements. The deep learning incorporated attention mechanism with MobileNetV2 as a base model utilizing Adam optimizer with ReLU activation achieved 99.23% accuracy, representing an outstanding result and indicating the model's effectiveness. It enhances the ability of the model to highlight necessary complex features within the GPR images and improves overall performance. The attention mechanism benefits from the self-attention mechanism, which enables it to conduct precise feature extraction. Figure 10 shows the comparison of the existing attention mechanism model with the proposed attention mechanism with MobileNetV2 as the base model for buried object classification. However, to prove the model's practical application in real situations, more research must include multiple datasets testing along with techniques to handle possible overfitting problems. Relating the attention mechanism with interpretability and feature significance enables researchers to acquire better insights about how the model arrives at its decisions.

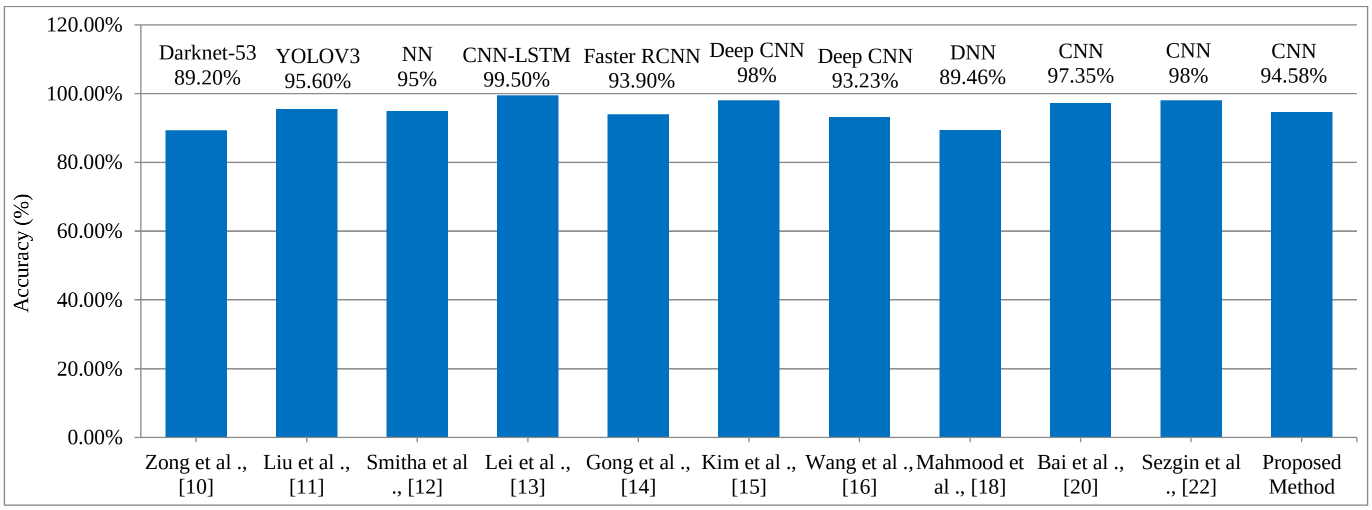

Fig. 9 Comparison of deep learning model for buried object classification

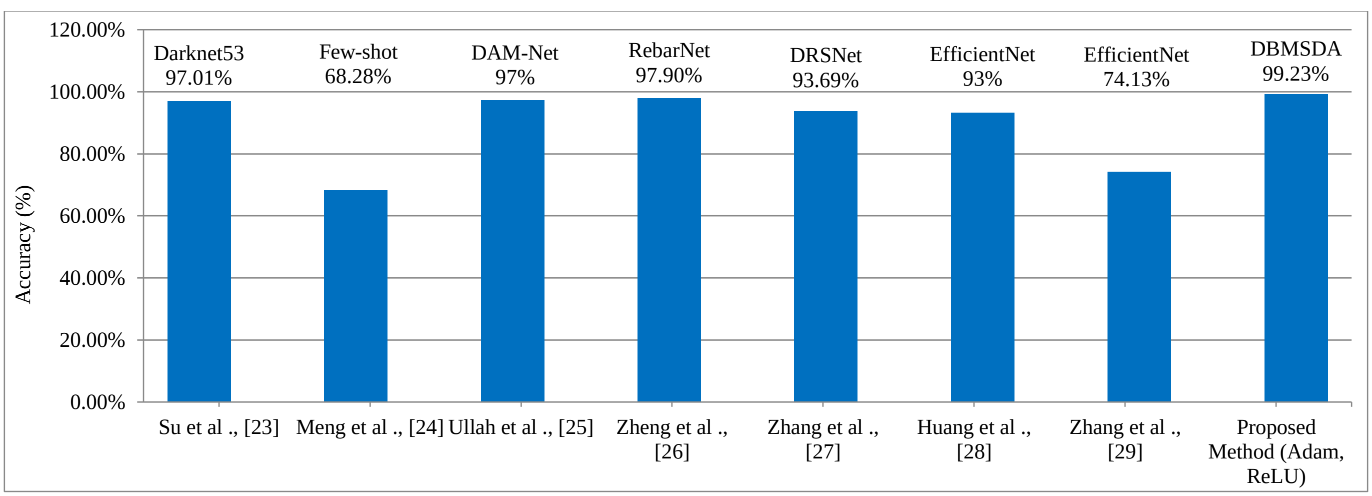

Fig. 10 Comparison of deep learning with an attention mechanism

7. Conclusion

The ground-penetrating radar images of buried objects classification model was developed using CNN and an attention mechanism. The CNN model achieved 94.58% accuracy in its multi-class classification. It shows the effectiveness of CNN in classifying GPR images of buried objects in varying subsurface conditions. Additionally, the deep learning employed MobileNetV2 with an attention mechanism achieved 99.23% accuracy.

The outstanding accuracy confirms that the model achieves superior performance when self-attention operates with MobileNetV2's efficient feature extraction mechanism to analyze intricate image features. The attention model can accurately classify buried objects like metal tiffin boxes, metal pipes, and plastic tiffin boxes from GPR B-scan images of simulated landmines, which enhances the safety of demining operations. The model is also useful in underground utility mapping to identify the presence of metallic or non-metallic-made cables and pipes that aid in infrastructure development, as well as applied in archaeological site assessment and geological applications to automate the detection, minimize human involvement, and speed up decision-making processes during real-world applications. Vision Transformers (ViTs) will improve the detection of long-range dependencies of landmines in future GPR B-Scan images. This will be achieved using multiple real-world and diverse terrain datasets to obtain promising results. Additionally, the research will enhance robustness by optimizing multi-head attention for different feature extractions.

Acknowledgments

Author 1 contributed to the concept and design and drafted the manuscript. Author 3 assisted in implementing the design. Author 2 reviewed the entire manuscript and design implementation and approved the final manuscript.

References

[1] Foreign Anti-Tank Landmine Kit-Inert Replicas, Inert Products LLC, 2023. [Online]. Available: https://inertproducts.com/product/inert-anti-tank-landmine-kit/

[2] Protecting Lives, ICBL/CMC, 2025. [Online]. Available: https://www.icblcmc.org/

[3] Anti-Personnel Landmines Convention, United Nations, 2019. [Online]. Available: https://disarmament.unoda.org/anti-personnel-landmines-convention/

[4] Landmine, Explosive Remnants of War (ERW), and Cluster Submunition Casualties in 2019, ReliefWeb, 2020. [Online]. Available: https://reliefweb.int/map/world/landmine-explosive-remnants-war-erw-and-cluster-submunition-casualties-2019

[5] Saman Ghaffarian et al., "Effect of Attention Mechanism in Deep Learning-Based Remote Sensing Image Processing: A Systematic Literature Review," *Remote Sensing*, vol. 13, no. 15, pp. 1-22, 2021. [CrossRef] [Google Scholar] [Publisher Link]

[6] Rudong Xu et al., "Attention-Mechanism-Containing Neural Networks for High-Resolution Remote Sensing Image Classification," *Remote Sensing*, vol. 10, no. 10, pp. 1-29, 2018. [CrossRef] [Google Scholar] [Publisher Link]

[7] Xiang Li et al., "Deep Learning Attention Mechanism in Medical Image Analysis: Basics and Beyonds," *International Journal of Network Dynamics and Intelligence*, vol. 2, no. 1, pp. 93-116, 2023. [CrossRef] [Google Scholar] [Publisher Link]

[8] Haoyuan Chen et al., "IL-MCAM: An Interactive Learning and Multi-Channel Attention Mechanism-Based Weakly Supervised Colorectal Histopathology Image Classification Approach," *Computers in Biology and Medicine*, vol. 143, 2022. [CrossRef] [Google Scholar] [Publisher Link]

[9] Fabio Giovanneschi et al., "Dictionary Learning for Adaptive GPR Landmine Classification," *IEEE Transactions on Geoscience and Remote Sensing*, vol. 57, no. 12, pp. 10036-10055, 2019. [CrossRef] [Google Scholar] [Publisher Link]

[10] Zeliang Zong et al., "A Deep Learning Approach for Urban Underground Objects Detection from Vehicle-Borne Ground Penetrating Radar Data in Real-Time," *The International Archives of the Photogrammetry, Remote Sensing and Spatial Information Sciences*, vol. 42, pp. 293-299, 2019. [CrossRef] [Google Scholar] [Publisher Link]

[11] Hai Liu et al., "Automatic Recognition and Localization of Underground Pipelines in GPR B-Scans Using a Deep Learning Model," *Tunnelling and Underground Space Technology*, vol. 134, 2023. [CrossRef] [Google Scholar] [Publisher Link]

[12] N. Smitha, and Vipula Singh, "Target Detection Using Supervised Machine Learning Algorithms for GPR Data," *Sensing and Imaging*, vol. 21, no. 1, pp. 1-15, 2020. [CrossRef] [Google Scholar] [Publisher Link]

[13] Wentai Lei et al., "Underground Cylindrical Objects Detection and Diameter Identification in GPR B-Scans Via the CNN-LSTM Framework," *Electronics*, vol. 9, no. 11, pp. 1-16, 2020. [CrossRef] [Google Scholar] [Publisher Link]

[14] Zhimin Gong, and Huaiqing Zhang, "Research on GPR Image Recognition Based on Deep Learning," *International Conference on Computer Science Communication and Network Security*, vol. 20, pp. 447-454, 2020. [CrossRef] [Google Scholar] [Publisher Link]

[15] Namgyu Kim et al., "A Novel 3D GPR Image Arrangement for Deep Learning-Based Underground Object Classification," *International Journal of Pavement Engineering*, vol. 22, no. 6, pp. 740-751, 2021. [CrossRef] [Google Scholar] [Publisher Link]

[16] Hui Wang et al., "Buried Target Detection Method for Ground Penetrating Radar Based on Deep Learning," *Journal of Applied Remote Sensing*, vol. 16, no. 1, pp. 1-21, 2022. [CrossRef] [Google Scholar] [Publisher Link]

[17] Maxwell M. Omwenga et al., "Cognitive GPR for Subsurface Object Detection Based on Deep Reinforcement Learning," *IEEE Internet Things Journal*, vol. 8, no. 14, pp. 11594-11606, 2021. [CrossRef] [Google Scholar] [Publisher Link]
[18] Safdar Mahmood et al., "Detecting Improvised Landmines Using Deep Neural Networks on GPR Image Dataset Targeting FPGAs," *2022 IEEE Nordic Circuits and Systems Conference*, Oslo, Norway, pp. 1-7, 2022. [CrossRef] [Google Scholar] [Publisher Link]
[19] Rakeeb Mohamed Jaufer et al., "A Preliminary Numerical Study to Compare the Physical Method and Machine Learning Methods Applied to GPR Data for Underground Utility Network Characterization," *Remote Sensing*, vol. 14, no. 4, pp. 1-17, 2022. [CrossRef] [Google Scholar] [Publisher Link]
[20] Xu Bai et al., "3D-GPR-RM: A Method for Underground Pipeline Recognition Using 3-Dimensional GPR Images," *Applied Sciences*, vol. 13, no. 13, pp. 1-22, 2023. [CrossRef] [Google Scholar] [Publisher Link]
[21] Tsukasa Mizutani, Jingzi Chen, and Shuto Yotsumoto, "The 3D Localization of Subsurface Pipes from Ground Penetrating Radar Images Using Edge Detection and Point Cloud Segmentation," *Measurement*, vol. 236, 2024. [CrossRef] [Google Scholar] [Publisher Link]
[22] Mehmet Sezgin, and Mahmut Nedim Alpdemir, "Classification of Buried Objects Using Deep Learning on GPR Data," *2023 IEEE International Conference on Advanced Systems and Emergent Technologies*, Hammamet, Tunisia, pp. 1-5, 2023. [CrossRef] [Google Scholar] [Publisher Link]
[23] Yang Su et al., "End-To-End Deep Learning Model for Underground Utilities Localization Using GPR," *Automation in Construction*, vol. 149, 2023. [CrossRef] [Google Scholar] [Publisher Link]
[24] Xiaoxia Meng et al., "Few-Shot Image Classification Algorithm Based on Attention Mechanism and Weight Fusion," *Journal of Engineering and Applied Science*, vol. 70, no. 1, pp. 1-14, 2023. [CrossRef] [Google Scholar] [Publisher Link]
[25] Zahid Ullah et al., "Densely Attention Mechanism Based Network for COVID-19 Detection in Chest X-Rays," *Scientific Reports*, vol. 13, no. 1, pp. 1-14, 2023. [CrossRef] [Google Scholar] [Publisher Link]
[26] Yanmei Zheng, Guanghui Zhou, and Bibo Lu, "A Multi-Scale Rebar Detection Network with an Embedded Attention Mechanism," *Applied Sciences*, vol. 13, no. 14, pp. 1-21, 2023. [CrossRef] [Google Scholar] [Publisher Link]
[27] XiaLin Zhang et al., "Rock Thin Section Image Classification Based on Depth Residuals Shrinkage Network and Attention Mechanism," *Earth Science Informatics*, vol. 16, no. 2, pp. 1449-1457, 2023. [CrossRef] [Google Scholar] [Publisher Link]
[28] Zhihao Huang et al., "Rock Image Classification Based on EfficientNet and Triplet Attention Mechanism," *Applied Sciences*, vol. 13, no. 5, pp. 1-20, 2023. [CrossRef] [Google Scholar] [Publisher Link]
[29] Heng Zhang et al., "Hyperspectral Image Classification Based on Double-Branch Multi-Scale Dual-Attention Network," *Remote Sensing*, vol. 16, no. 12, pp. 1-29, 2024. [CrossRef] [Google Scholar] [Publisher Link]
[30] Ge Junkai et al., "GPR-TransUNet: An Improved TransUNet Based on Self-Attention Mechanism for Ground Penetrating Radar Inversion," *Journal of Applied Geophysics*, vol. 222, 2024. [CrossRef] [Google Scholar] [Publisher Link]